

ORIGINAL RESEARCH ARTICLE

Prognostic implication and oncogenic role of *DDIT3* in breast cancer

Fajia Yuan¹, Lirong Jia², Jin Jin², Yuezhen Liu², Xiaojun Cao², and Hui Li^{3*}

¹Department of Medical and Health, Jin Zhong Vocational and Technical College, Jinzhong, Shanxi, China

²Department of Basic Medicine, Jin Zhong Health School, Jinzhong, Shanxi, China

³Shanxi Bethune Hospital, Shanxi Academy of Medical Sciences, Tongji Shanxi Hospital, Third Hospital of Shanxi Medical University, Taiyuan, Shanxi, China

Abstract

Although DNA damage-inducible transcript 3 (*DDIT3*) has been identified as a novel gene associated with breast cancer, its clinical significance, biological function, and underlying mechanisms remain unclear. By integrating immunohistochemistry with data from The Cancer Genome Atlas (TCGA), we discovered that elevated levels of *DDIT3* Messenger RNA and protein expression are significantly associated with poor prognosis in patients with breast cancer. Functional assays and preliminary mechanistic studies reveal that *DDIT3* may promote breast cancer cell proliferation and metastasis, potentially by downregulating activating transcription factor-2.

Keywords: Breast cancer; *DDIT3*; Prognosis; Oncogene

*Corresponding author:

Hui Li
(415310418@qq.com)

Citation: Yuan F, Jia L, Jin J, Liu Y, Cao X, Li H. Prognostic implication and oncogenic role of *DDIT3* in breast cancer. *Cancer Plus*. 2026;8(1):025100014.
doi: 10.36922/CP025100014

Received: March 6, 2025

1st revised: April 12, 2025

2nd revised: April 20, 2025

3rd revised: April 23, 2025

4th revised: April 28, 2025

5th revised: June 14, 2025

Accepted: June 24, 2025

Published online: February 24, 2026

Copyright: © 2026 Author(s). This is an Open-Access article distributed under the terms of the Creative Commons Attribution License, permitting distribution, and reproduction in any medium, provided the original work is properly cited.

Publisher's Note: AccScience Publishing remains neutral with regard to jurisdictional claims in published maps and institutional affiliations.

1. Introduction

Breast cancer remains one of the most significant public health challenges worldwide, ranking as the second leading cause of cancer-related mortality and the most frequently diagnosed malignancy among women, accounting for approximately 30% of all female cancer cases.¹ In 2020, China reported 4.57 million new cancer cases and 3 million deaths, ranking first globally. Breast cancer incidence in China is rising at rates significantly exceeding the global average.^{1,2} Compared with European and American countries, China has a higher proportion of young breast cancer patients, a younger age of onset, and a later clinical stage at diagnosis. The proportion of early-stage cases and survival rates is significantly lower than those observed in European and American countries.^{3,4} This disparity may be attributed to factors such as denser breast anatomy among Chinese women, population aging, genetic predisposition, and other factors.⁵⁻⁷ These differences imply that breast cancer may exhibit substantial heterogeneity across races, countries, and regions, and therefore, the direct application of foreign research findings to the diagnosis and treatment of breast cancer in China may lack the precision required for personalized medicine. Existing serum tumor markers (CA153, carcinoembryonic antigen) have critical shortcomings, including suboptimal sensitivity and specificity, limited clinical utility for early detection, and inadequate prognostic value.^{8,9} Therefore, identifying novel, population-relevant biomarkers for breast cancer and elucidating molecular mechanisms specific to Chinese patients are essential for developing precise diagnostic tools for early detection, accurate prognosis prediction, and targeted therapeutic strategies.

DNA damage-inducible transcript 3 (*DDIT3*), also known as *GADD153*, encodes a stress-inducible transcription factor that serves as a critical molecular switch governing cell fate under diverse pathological conditions.¹⁰ As a member of the CCAAT/enhancer-binding protein (C/EBP) family, *DDIT3* exhibits unique functional characteristics. It is robustly activated by various cellular stresses, including endoplasmic reticulum (ER) stress, oxidative stress, hypoxia, and DNA damage, and orchestrates the balance between cell survival and apoptosis through modulation of downstream effectors such as B-cell lymphoma 2 family proteins and autophagy-related genes.^{11,12} Beyond its role in stress responses, *DDIT3* participates in adipocyte differentiation and lipid metabolism through regulation of peroxisome proliferator-activated receptor gamma,¹³ cardiac remodeling by modulating cardiomyocyte apoptosis,¹⁴ and neural development and synaptic plasticity.¹⁵ Emerging evidence reveals that *DDIT3* has a complex, cancer-type-specific role. In hematological malignancies, *DDIT3* induces ER stress-mediated apoptosis, making it a potential therapeutic target.¹⁶ In solid tumors, *DDIT3* may promote tumor cell adaptation to microenvironmental stress,¹⁷ epithelial-mesenchymal transition and metastasis,¹⁸ and chemoresistance through stress-response pathways.¹⁹ In breast cancer, *DDIT3* has traditionally been viewed as a mediator of therapy-induced apoptosis.²⁰ However, its role in regulating breast cancer progression remains largely unexplored. Moreover, although *DDIT3* has been implicated in therapy resistance, its prognostic significance and potential pro-metastatic role in breast cancer have not been previously characterized and are newly demonstrated in this study. This study addresses a critical knowledge gap by elucidating how stress-response pathways contribute to breast cancer pathogenesis and highlighting novel avenues for targeted interventions.

2. Materials and methods

2.1. Cell culture

Human breast cancer cell lines Michigan cancer foundation (MCF7) and Hs578T were obtained from Shanxi Bethune Hospital. Cells were cultured in Roswell Park Memorial Institute (RPMI) 1640 medium (Biological Industries, Israel) supplemented with 10% fetal bovine serum (Biological Industries, Israel) and 1% penicillin/streptomycin (Hyclone, USA) and maintained in a humidified incubator (371GPCN, Thermo Fisher, USA) at 37°C with 5% CO₂. On reaching 80–90% confluence, the cells in the logarithmic growth phase were harvested for subsequent experiments.

2.2. Cell transfection

When cells in 6-well plates reached 60–80% confluence, they were transfected with small interfering RNA (siRNA) targeting *DDIT3* and negative control siRNA (siRNA-NC) using Lipofectamine 2000 (Invitrogen, USA), following the manufacturer's instructions. Briefly, 125 µL Opti-MEM reduced-serum medium (Thermo Fisher, USA), 5 µL Lipofectamine 2000, and 5 µL siRNA-*DDIT3* or siRNA-NC were combined in a sterilized Eppendorf (EP) tube, mixed gently, and incubated for 20 min at room temperature. Subsequently, the resulting complexes were added to each well containing complete medium without antibiotics, and cells were cultured in a humidified incubator at 37°C with 5% CO₂, protected from light. Digested cells were subjected to functional assays after 48 h. siRNA-*DDIT3* and siRNA-NC were purchased from RiBio (China). The siRNA sequence targeting *DDIT3* was: 5'-CGGAAACAGAGUGGUCAUUt-3'.

2.3. Cell counting kit-8 (CCK-8) assay

Transfected cells were digested and resuspended to form a single-cell suspension. Cells were seeded into 96-well plates at a density of 5×10^3 cells/well and incubated overnight under normal conditions. Cell viability was assessed at 24, 48, 72, and 96 h by adding 10 µL CCK-8 solution (SEVEN Biotech, China) to each well, followed by incubation at 37°C for 1 h. Absorbance was measured at 450 nm with a microplate reader (Synergy LX, BioTek, USA). Each experiment was repeated at least 3 times.

2.4. Transwell assay

After dilution of human breast cancer cells with RPMI 1640 medium, 200 µL of cell suspension was inoculated into the upper chamber (5×10^4 cells/well) of a Transwell insert (Corning, USA), and RPMI 1640 medium containing 10% fetal bovine serum (600 µL) was added to the lower chamber of a 24-well plate. After 24 h of incubation at 37°C with 5% CO₂, non-migrated cells remaining on the upper surface of the membrane were removed with a cotton swab. Migrated cells on the lower surface were fixed with 4% paraformaldehyde (Sangone Biotech, China) for 15 min, stained with 0.1% crystal violet (Sangone Biotech, China) for 15 min, and photographed under an inverted fluorescence microscope (Olympus Corporation, Japan). The number of migrated cells was counted in 10 randomly selected fields per insert.

2.5. Colony formation assay

Cells were seeded into 6-well plates at a density of 500 cells per well in complete RPMI-1640 medium and cultured for 2 weeks. On the 14th day, cells were fixed with 4%

paraformaldehyde and stained with 1% crystal violet, and then manually counted under a microscope.

2.6. Real-time quantitative polymerase chain reaction (qPCR)

Total RNA was extracted using TRIzol reagent (Takara Biotech, Japan) according to the manufacturer's instructions. Briefly, cells were lysed in 1 mL Trizol at room temperature for 5 min, followed by the addition of 200 μ L chloroform. After vigorous mixing and centrifugation at 12,000 rpm for 15 min at 4°C, the supernatant was collected into a new clean 1.5 mL EP tube. RNA was precipitated with an equal volume of isopropanol (Tianli Chem, China) at -20°C for 30 min and centrifuged at 12,000 rpm for 10 min at 4°C. The supernatant was discarded, and the RNA pellet was washed with 1 mL of 70% ethanol solution treated with diethyl pyrocarbonate (Sangone Biotech, China), air-dried for 3–5 min, and resuspended in 30–50 μ L RNase-free water (Sangone Biotech, China). RNA concentration and purity were assessed using a NanoDrop 2000 spectrophotometer (Thermo Fisher Scientific, USA) by measuring absorbance at 230, 260, and 280 nm. RNA samples with an A260/A280 ratio of 1.8–2.0 and an A260/A230 ratio >2.0 were considered acceptable for subsequent experiments. Reverse transcription was performed according to the manufacturer's instructions using 5 \times PrimeScript RT Master Mix (Takara Biotech, Japan) with 2 μ g total RNA and RNase-free water in a final volume of 20 μ L. Reverse transcription was performed at 37°C for 15 min, 85°C for 15 min, and 4°C hold for 5 s. qPCR was performed using the SYBR Green chemistry on an SLAN-96P Real-Time PCR Detection System (Hongshi Biotech, China). Cycling conditions were 95°C for 10 min, followed by 40 cycles of 95°C for 15 s and 60°C for 15 s. The housekeeping gene (glyceraldehyde-3-phosphate dehydrogenase [GAPDH]) was used as the internal control, and relative expression was calculated by the $\Delta\Delta C_t$ method. Primers were purchased from SangonCo., Ltd (Shanghai, China). Primer sequences were as follows:

- (i) DDIT3: F 5'-CATTGCCTTTCTCCTTCGGG-3', R 5'-CCAGAGAAGCAGGGTCAAGA-3'
- (ii) GAPDH: F 5'-CCAGAACATCATCCCTGCCT-3', R 5'-CCTGCTTCACCACTTCTTG-3'
- (iii) Activating transcription factor-2 (ATF2): F 5'-CTGTAATCACCCAGGCACCA-3', R 5'-TTCGAAGCATGCACACACATAC-3'

2.7. Western blot

Total protein was extracted using RIPA lysis buffer supplemented with protease and phosphatase inhibitors (Beyotime, China). Protein concentrations were quantified using a bicinchoninic acid assay (Beyotime, China). Equal

amounts of protein (50 μ g) were separated by sodium dodecyl sulfate–polyacrylamide gel electrophoresis on 10% polyacrylamide gels (SEVEN Biotech, China) and transferred onto polyvinylidene difluoride membranes (Millipore, Germany) using a wet transfer system at 80 V for 120 min. Membranes were blocked with 5% non-fat milk (SEVEN Biotech, China) in Tris-buffered saline with Tween 20 (TBST) (Yeasen Biotech, China) for 1 h at room temperature and incubated overnight at 4°C with primary antibodies against DDIT3 (1:1000) and ATF2 (1:500) (Proteintech, USA). GAPDH (1:50,000; Proteintech, USA) was used as the loading control. After washing 3 times with TBST, membranes were probed with horseradish peroxidase-conjugated secondary antibodies (1:5000 dilution; Cell Signaling Technology, USA) for 1 h at room temperature. Protein bands were visualized using enhanced chemiluminescence (ECL Prime) (Amersham, UK) and imaged with a ChemiDoc MP Imaging System (Bio-Rad, USA). Band intensities were quantified and normalized to GAPDH.

2.8. Immunohistochemistry

A tissue microarray (TMA) containing 140 breast cancer specimens (stage I–IIIC) was purchased from Shanghai Xinchao Biotechnology Co., Ltd (China). The tissue sections were baked at 70°C for 2 h in advance, followed by deparaffinization in 100% xylene solution (three changes, 10 min each) (Tianli Chem, China) and rehydration through a graded descending ethanol series (95%, and 75%, 5 min each). Endogenous peroxidase activity was blocked by immersing the sections in 3% hydrogen peroxide (Tianli Chem, China) for 20 min in the dark, and the sections were quickly washed with three washes of distilled water. Antigen retrieval was performed by heating sections in sodium citrate buffer (pH 6.0) (Roles-Bio, China) at boiling temperature for 2.5 min and maintaining the temperature for an additional 5 min. After cooling to room temperature, sections were washed with 1 \times phosphate-buffered saline (Roles-Bio, China) 3 times for 5 min each and blocked with 2% goat serum (Zhong Shan Gold Bridge Biotech, China) at 37°C for 20 min. Sections were then incubated overnight at 4°C with the DDIT3 primary antibody diluted with phosphate-buffered saline with Tween-20 (PBST) (Yeasen Biotech, China). Sections incubated with PBST alone served as negative controls. The following day, the wet box containing the sections was transferred to room temperature, rewarmed for 1 h, and washed 3 times with PBST for 5 min. Sections were incubated with a fast enzyme-labeled polymer secondary antibody (anti-mouse/rabbit immunoglobulin G) (Zhong Shan Gold Bridge Biotech, China) at 37°C for 20 min, and washed 3 times with PBST, 5 min each. 3,3'-diaminobenzidine (HARVEYBIO, China) was added dropwise until the cytoplasm became pale

yellow, and the color reaction was terminated with distilled water. The sections were counterstained with hematoxylin (Beyotime Biotech, China) for 1 min, differentiated in hydrochloric acid alcohol (Tianli Chem, China) for 2 s, blued in ammonia water (Tianli Chem, China) for 52 s, and rinsed with distilled water. Sections were dehydrated through a graded ascending ethanol series (75% ethanol and 95%, 5 min each), cleared in 100% xylene solution (three changes for 10 min each), air-dried, and mounted with neutral resin (Beyotime Chem, China). The TMA and the expression of cytoplasmic proteins were scanned and analyzed by the 3D Histech tissue scanning analysis system (3D Histech, Hungary). Statistical analyses were performed using Statistical Package for the Social Sciences (SPSS) 26.0 software.

2.9. Data preprocessing and standardization pipeline

Publicly available RNA sequencing and clinical data for breast cancer were obtained from TCGA cohort (Project ID: TCGA-BRCA; Data Version GDC Release 32). Raw RNA-seq expression matrices (Fragments Per Kilobase of transcript per Million mapped reads [FPKM] format) and corresponding clinical survival information were downloaded from the Genomic Data Commons Data Portal. Data preprocessing was conducted as follows: (i) Sample filtering: Samples with overall survival (OS) ≤ 30 days, to minimize the inclusion of non-cancer-related deaths, and samples with incomplete clinical information were excluded, resulting in 773 eligible cases for subsequent analyses. (ii) Gene expression filtering: The “filterByExpr()” function from the edgeR package (v3.40.2) was applied to retain genes expressed at >1 FPKM in $\geq 50\%$ of samples. (iii) Missing value handling: No missing values were detected in the gene expression matrix. (iv) Normalization and transformation: Variance-stabilizing transformation was applied using the “varianceStabilizingTransformation()” function in “DESeq2” (v1.38.3) to mitigate sequencing depth bias. Batch effects associated with sequencing centers (Biospecimen Core Resource) were corrected using sva: ComBat (v3.48.0) while preserving biological signals (mean.only = FALSE).

2.10. Statistical analysis

Patients were stratified into *DDIT3*-high and *DDIT3*-low expression groups based on median *DDIT3* expression levels. Survival outcomes were analyzed using Kaplan-Meier curves, and differences in the OS between *DDIT3* expression groups were assessed using log-rank tests. OS was analyzed both for the entire cohort and across clinicopathological subgroups. Cause-of-death determinations were verified using national death registry linkages based on the

International Classification of Diseases, 10th Revision (C50 for breast cancer-specific mortality). The primary endpoint was defined as breast cancer-specific death. Censoring events included (i) right-censoring for patients alive at the end of follow-up or lost to follow-up, and (ii) competing-risk censoring for deaths due to causes other than breast cancer. Cox proportional hazards regression analyses were performed to assess prognostic factors, with hazard ratios (HRs) and 95% confidence intervals reported. Continuous variables were compared using independent two-sample *t*-tests (mean \pm SD). Bivariate correlations were evaluated through Pearson's coefficient (*r*). All analyses were performed in SPSS version 26.0 (IBM Corp, USA), with a two-tailed $p < 0.05$ considered statistically significant. All *in vitro* experiments were performed with at least three independent biological replicates per condition ($n \geq 3$ per condition) to ensure reproducibility.

3. Results

3.1. High expression of *DDIT3* protein is associated with poor prognosis in breast cancer patients

Using immunohistochemistry on a TMA containing 140 breast cancer specimens, we observed that *DDIT3* protein was predominantly expressed in the cytoplasm of breast cancer cells (Figure 1A). Based on the median expression score of the *DDIT3* protein, we divided breast cancer cases into *DDIT3*_{high} and *DDIT3*_{low} groups. Kaplan-Meier survival analysis showed that the OS of breast cancer patients with high expression of *DDIT3* protein was shorter than that of patients with low expression, suggesting that high expression of *DDIT3* protein was associated with poor prognosis of breast cancer patients (Figure 1B).

3.2. High expression of *DDIT3* messenger RNA (mRNA) is associated with poor prognosis in breast cancer patients

Breast cancer cases from the TCGA cohort were analyzed, and the samples were divided into *DDIT3*_{high} and *DDIT3*_{low} groups according to an optimal cutoff value (cutoff value = 7.4820) derived from receiver operating characteristic curves of *DDIT3* mRNA expression. Survival analysis showed that breast cancer patients with high *DDIT3* mRNA expression exhibited significantly shorter OS compared with those with low expression ($p < 0.05$) (Figure 2A). Stratified analyses based on clinicopathological factors further showed that the survival time of patients with high *DDIT3* mRNA expression was shorter than that of patients with low *DDIT3* expression in patients older than 60 years ($p < 0.05$), those with Tumor, Node, Metastasis (TNM) stage I+II ($p < 0.01$), pathological T3+4 tumors ($p < 0.05$), absence of lymph node metastasis ($p < 0.05$), estrogen receptor-positive (ER+) tumors

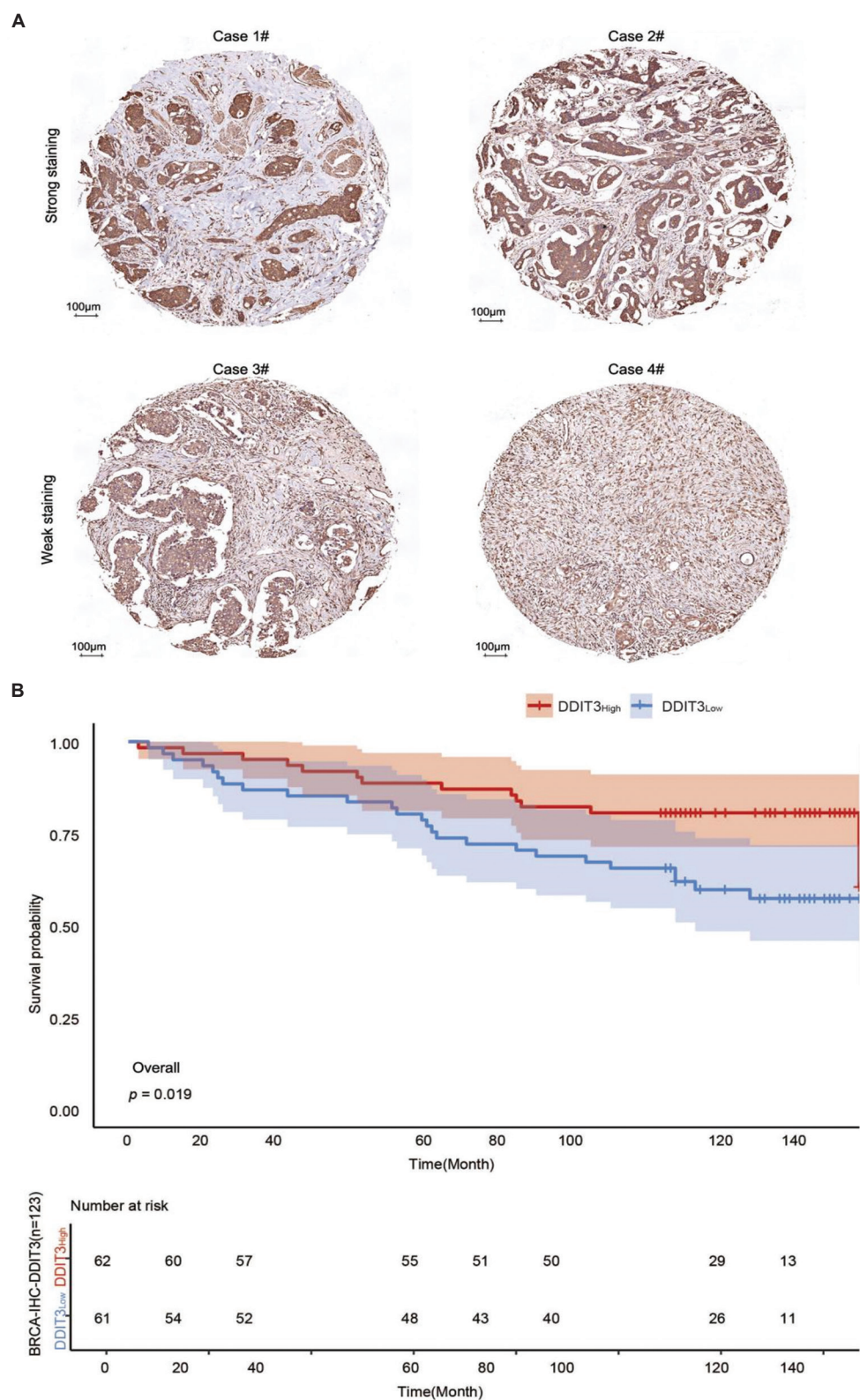


Figure 1. Prognostic value of DNA damage-inducible transcript 3 (DDIT3) protein expression in breast cancer patients. (A) Representative immunohistochemistry images showing DDIT3 expression in breast cancer tissues from a tissue microarray containing 140 formalin-fixed, paraffin-embedded tumors. Scale bars: 100 µm; magnification: ×7.4. (B) Kaplan-Meier overall survival curves stratified by DDIT3 protein expression levels in all breast cancer patients.

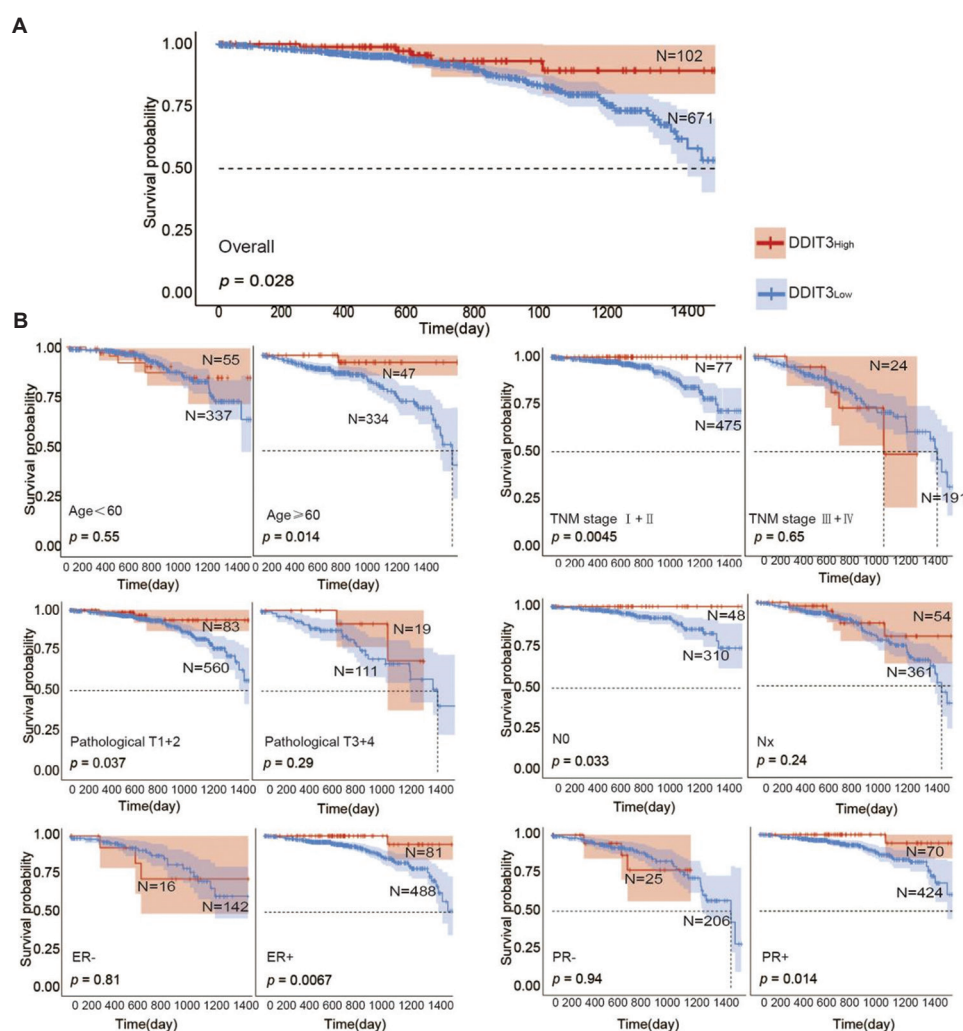


Figure 2. Prognostic value of DNA damage-inducible transcript 3 (*DDIT3*) messenger RNA (mRNA) expression in breast cancer patients. (A) Kaplan-Meier overall survival curves stratified by *DDIT3* mRNA expression in the overall breast cancer cohort. (B) Kaplan-Meier overall survival curves stratified by *DDIT3* mRNA expression across clinicopathological subgroups, including age, lymph node metastasis status, tumor, node, metastasis stage, pathological T stage, and estrogen receptor and progesterone receptor expressions.

($p < 0.01$) and progesterone receptor-positive (PR+) tumors ($p < 0.05$) (Figure 2B).

3.3. High expression of *DDIT3* mRNA is a risk factor for survival of breast cancer patients

To evaluate the prognostic value of *DDIT3* mRNA expression for the cumulative survival of breast cancer patients, univariate Cox proportional hazard regression analysis was performed. The results showed that, in addition to lymph node metastasis (HR: 0.421, 95% CI: 0.261–0.679, $p < 0.001$), pathological T stage (HR: 0.405, 95% CI: 0.256–0.639, $p < 0.001$), and TNM stage (HR: 0.300, 95% CI: 0.196–0.460, $p < 0.001$), high *DDIT3* mRNA expression was also an important risk factor affecting OS status (HR: 0.375, 95% CI: 0.151–0.931, $p = 0.034$) (Figure 3).

3.4. The decreased expression of *DDIT3* can inhibit the proliferation, migration, and colony formation of breast cancer cells

MCF7 and Hs578T breast cancer cell lines were selected for interference experiments. The interference efficiency was confirmed by qPCR and Western blot analysis (Figure 4A and B, Figure A1A). It was found that the interference efficiency of *DDIT3* exceeded 70% in both cell lines. The results of the CCK-8, colony formation, and Transwell assays showed that transfection of *DDIT3* siRNA significantly inhibited breast cancer cell proliferation ($p < 0.01$), migration ($p < 0.01$), and colony formation ability of breast cancer cells ($p < 0.01$) (Figure 4C-E).

3.5. ATF2 may be a direct downstream target gene of DDIT3

Potential downstream target genes of *DDIT3* were predicted using the transcriptional regulatory relationships

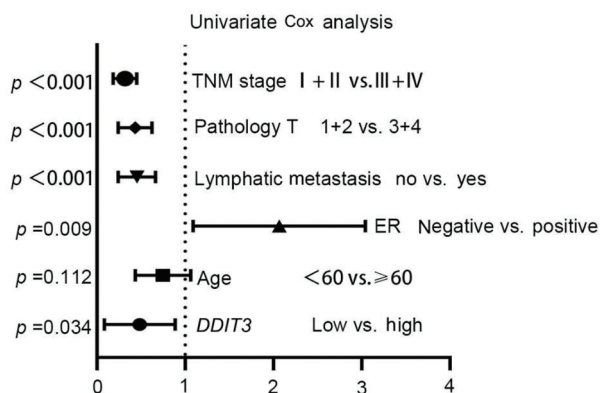


Figure 3. Univariate analysis by Cox proportional hazards regression analysis of overall survival in the overall breast cancer cohort

unrevealed by sentence-based text (TRRUST) mining database (<https://ngdc.cncb.ac.cn/databasecommons/database>), yielding 18 candidate genes (Figure 5A). Among these, the promoter activities of *ANKRD1*, *ASNS*, *ATF2*, *ATF5*, *CEBPA*, *NOS3*, *SIRT1*, and *SIRT2* were predicted to be inhibited, and the promoter activities of *ATG5*, *IL6*, *MAP1LC3 B*, *RTN3*, and *TRIB3* were predicted to be activated. The regulatory effects of *DDIT3* on *TNFRSF10B*, *CDK2*, *CXCL8*, *TF*, and *MCL1* promoter activity remain unclear. Subsequent analysis of the TCGA breast cancer expression dataset revealed a significant negative correlation between *ATF2* and *DDIT3* expression ($r = -0.4038$, $p < 0.001$) (Figure 5B). Consistent with the observed inhibition of *ATF2* promoter activity, qPCR and Western blot analyses further confirmed the regulatory relationship between *DDIT3* and *ATF2* (Figures 5C and D and Figure A1B). These results collectively suggest that *DDIT3* likely contributes to breast cancer pathogenesis and progression by modulating *ATF2* expression, as illustrated in the proposed mechanistic model (Figure 5E).

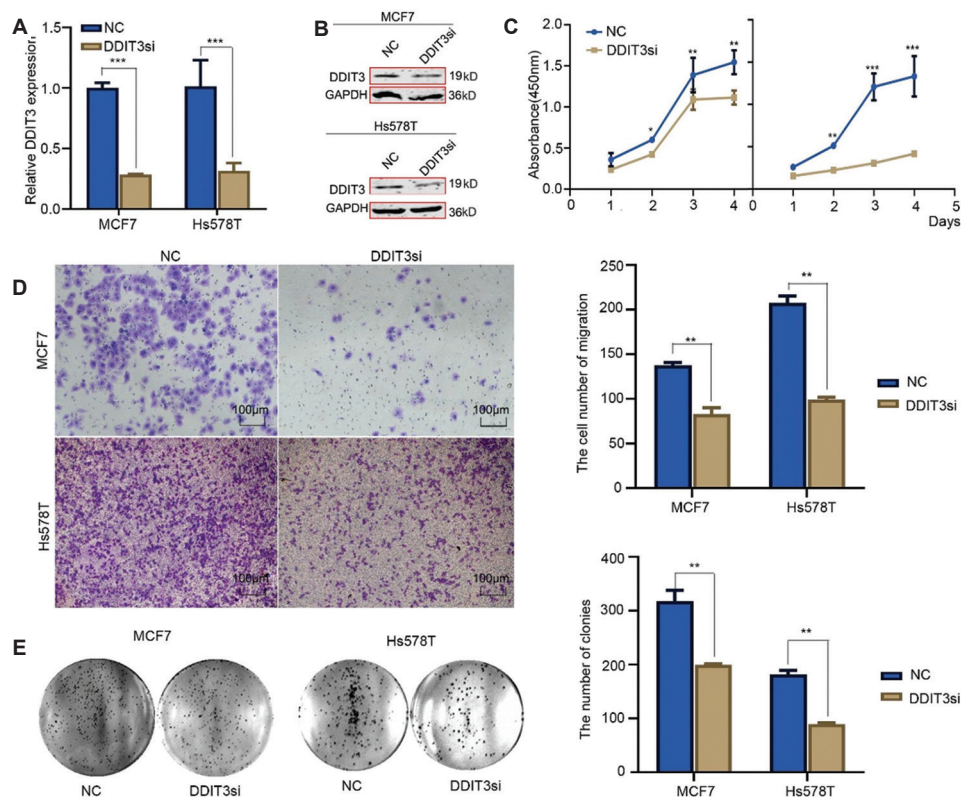


Figure 4. DNA damage-inducible transcript 3 (*DDIT3*) acts as an oncogene affecting breast cell growth, colony formation, and cell migration. (A and B) Knockdown efficiency of *DDIT3* in MCF7 and Hs578T cells was confirmed by quantitative polymerase chain reaction and Western blot. (C) Cell counting kit-8 assay showed that *DDIT3* knockdown significantly inhibited the proliferation of breast cancer cells. (D) Transwell assays demonstrated that *DDIT3* knockdown markedly reduced breast cancer cell migration. Scale bar: 100 μ m. (E) Colony formation assays revealed a significant decrease in the number of colonies in the *DDIT3* knockdown group compared to the control.

Notes: All data are presented as mean \pm standard deviation from three independent experiments. * $p < 0.05$, ** $p < 0.01$, and *** $p < 0.001$

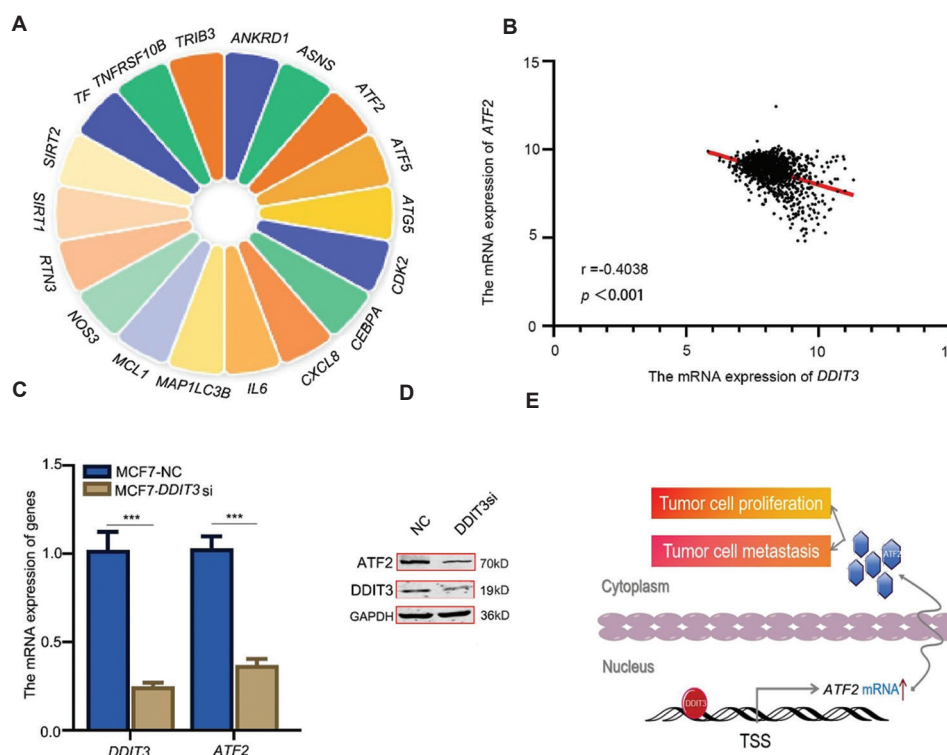


Figure 5. Negative correlation between DNA damage-inducible transcript 3 (*DDIT3*) and activating transcription factor 2 (*ATF2*) expression in breast cancer. (A) Predicted downstream target genes of *DDIT3* based on the transcriptional regulatory relationships unraveled by sentence-based text database. (B) Correlation analysis of *ATF2* and *DDIT3* expression in breast cancer samples from the Cancer Genome Atlas database. (C and D) *DDIT3* and *ATF2* expression levels were assessed by quantitative polymerase chain reaction and Western blot. (E) Proposed schematic model illustrating the regulatory relationship between *DDIT3* and *ATF2* in breast cancer.

Notes: * $p < 0.05$, ** $p < 0.01$, and *** $p < 0.001$.

4. Discussion

Emerging evidence positions *DDIT3* as a critical mediator of therapeutic resistance and tumor aggressiveness across multiple malignancies. *DDIT3* dysregulation has been associated with ECL through activation of stress-adaptation pathways;¹⁷⁻¹⁹ accordingly, elevated *DDIT3* expression has been linked to poor prognosis in some cancers. Similarly, *DDIT3* has been used as an independent prognostic predictor in melanoma and early-stage non-small cell lung cancer.^{21,22} Consistent with these findings, elevated *DDIT3* expression has also been correlated with poor clinical outcomes in gastric cancer, where tumor tissues exhibit a 2.3-fold increase compared with normal tissues.²³ High *DDIT3* levels are also associated with reduced median survival in advanced gastric cancer.²⁴ Despite these advances, the clinical significance and molecular mechanisms of *DDIT3* in breast cancer have remained largely unexplored. In the present study, immunohistochemical analysis of a TMA containing 140 cases revealed that cytoplasmic overexpression of *DDIT3* was significantly correlated with reduced 5-year OS and advanced TNM stage. In addition,

analysis of the TCGA breast cancer cohort showed that high *DDIT3* mRNA expression predicted poorer prognosis in patients aged over 60 years, as well as in ER+, PR+, TNM stage I + II, pathological T3 + 4, and lymph node-negative metastasis subgroups. To further confirm the predictive value of *DDIT3* for OS in breast cancer patients, univariate Cox proportional hazard regression analysis was performed. Both univariate and multivariate analyses identified *DDIT3* as an independent prognostic factor for OS, alongside established clinicopathological parameters such as lymph node metastasis and TNM stage.

In current clinical practice, prognostic evaluation of breast cancer primarily relies on well-established biomarkers, including the Ki-67 proliferation index, ER/PR/human epidermal growth factor receptor 2 (HER2) status, and multigene assays such as Oncotype DX. Although Ki-67 is a marker of cellular proliferation, its clinical utility is limited by interobserver variability and dynamic changes in expression during treatment. In contrast, *DDIT3* exhibits more stable expression patterns in archival tissue specimens and may better capture

stress-induced tumor adaptation mechanisms. Unlike ER/PR/HER2 status, which primarily informs subtype classification and targeted therapeutic strategies, *DDIT3* provides orthogonal prognostic information independent of hormone receptor signaling, potentially enabling the identification of high-risk subsets within luminal breast cancer. Compared with multigene assays such as Oncotype DX, which integrates 21 genes to predict recurrence risk and chemotherapy benefit, *DDIT3* offers a cost-effective single-gene biomarker while retaining prognostic granularity. Notably, our findings suggest that integrating *DDIT3* with Oncotype DX may further improve risk stratification accuracy, suggesting potential synergistic clinical utility. However, the clinical translation of *DDIT3* as a prognostic marker requires further validation against gold-standard multigene assays across diverse populations. In addition, standardized detection protocols and dynamic monitoring of *DDIT3* expression during therapy should be explored to fully define the clinical utility relative to existing established biomarkers.

DDIT3 has been reported to promote cancer stem cell stemness by upregulating *CEBPB* in gastric cancer.²⁴ As a transcription factor, *DDIT3* can mediate the transcription of *BBC3* and *BCL2L11*,²⁵ as well as the transcription of *TNFRSF10B* to participate in the apoptosis process induced by ER stress.²⁶ Recent studies have shown that *DDIT3* can directly or indirectly regulate multiple autophagy-related genes, contributing to the pro-survival processes mediated by autophagy.²⁷ Therefore, to clarify the function of *DDIT3* in breast cancer, we conducted a preliminary exploration of functional experiments. Knockdown of *DDIT3* in MCF7 and Hs578T cell lines led to significant reductions in cell proliferation, colony formation, and migration of breast cancer cells, as assessed by CCK-8, colony formation assay, and Transwell assay, suggesting that *DDIT3* may act as an oncogene in breast cancer.

DDIT3 can function both as an inhibitor of the nuclear transcription factor *C/EBPβ*²⁸ and as an activator of other genes. In non-small cell lung cancer, *DDIT3* mediates *TNFRSF10A*-dependent apoptosis in response to ER stress inducers.²⁹ Additionally, *DDIT3* has been reported to degrade electron transport chain proteins COQ9 and COX4, through mitochondria hydrolase *LONP1*, thereby inhibiting mitochondrial oxidative phosphorylation and reducing the excessive reactive oxygen species production.³⁰ Therefore, to investigate the specific mechanism by which *DDIT3* contributes to breast cancer, we used the TRRUST database to predict downstream targets and identified 18 putative target genes with *DDIT3*-responsive promoters. Among these, the promoter activities of *ANKRD1*, *ASNS*, *ATF2*, *ATF5*, *CEBPA*, *NOS3*, *SIRT1*, and *SIRT2* were

predicted to be inhibited, and the promoter activities of *ATG5*, *IL6*, *MAP1LC3B*, *RTN3*, and *TRIB3* were predicted to be activated. However, the regulatory effects on *TNFRSF10B*, *CDK2*, *CXCL8*, *TF*, and *MCL1* promoter activity remain unknown. Furthermore, correlation analysis using TCGA data showed a significant inverse association between *DDIT3* and *ATF2* expression, which was consistent with the TRRUST prediction. Therefore, we speculate that *DDIT3* may promote the development of breast cancer by directly inhibiting *ATF2* promoter activity.

ATF2, a DNA-binding protein of the leucine zipper family, regulates apoptosis via p53 stabilization³¹ and inhibits metastasis through the downregulation of *MMP9*.³² Loss of *ATF2* expression correlates with 32% shorter disease-free survival in ER+ breast cancer and supports its role as a tumor suppressor in breast cancer.

5. Conclusion

Taken together, our findings identify *DDIT3* as a pathological master regulator of breast cancer progression, validate its potential clinical utility as an independent prognostic biomarker, and unveil the *DDIT3*-*ATF2* transcriptional axis as a potentially druggable vulnerability for targeted therapeutic intervention. Translational applications could include the incorporation of *DDIT3* protein detection via immunohistochemistry staining into routine pathological reporting for breast cancer or the development of prognostic scoring models integrating *DDIT3* mRNA and *ATF2* expression levels. However, clinical translation faces three critical challenges, including the standardization of detection protocols, mechanistic complexity, and ensuring therapeutic safety. Advancing companion diagnostics and optimizing targeted delivery technologies may accelerate the translation of these findings from “bench to bedside.” This study has several limitations. The generalizability of *DDIT3* as a prognostic biomarker is constrained by reliance on a single TCGA dataset and an institutional TMA cohort. Further validation using independent datasets, such as the Molecular Taxonomy of Breast Cancer International Consortium or Gene Expression Omnibus, is warranted to strengthen the evidence base and provide a solid foundation for clinical translation of *DDIT3*.

Acknowledgments

None.

Funding

This work was financially supported by the Science and Technology Innovation Project of Universities in Shanxi (2021RC010); Shanxi Bethune Hospital National Natural Seed Players Cultivation Project (2023GZRZ22); Basic

Research Program of Shanxi Province (202403021211182); and the Research and Innovation Team Project for Scientific Breakthroughs at Shanxi Bethune Hospital (2024AOXIANG04).

Conflict of interest

The authors declare that they have no competing interests.

Author contributions

Conceptualization: Hui Li

Formal analysis: Lirong Jia, Yuezheng Liu, Xiaojun Cao

Investigation: Hui Li

Methodology: Fajia Yuan, Jin Jin

Writing – original draft: Fajia Yuan

Writing – review & editing: Hui Li

Ethics approval and consent to participate

Not applicable.

Consent for publication

Not applicable.

Availability of data

The data used in this study are available from the corresponding author on reasonable request.

References

- Bray F, Laversanne M, Sung H, *et al.* Global cancer statistics 2022: GLOBOCAN estimates of incidence and mortality worldwide for 36 cancers in 185 countries. *CA Cancer J Clin.* 2024;74(3):229-263.
doi: 10.3322/caac.21834
- Sung H, Ferlay J, Siegel RL, *et al.* Global cancer statistics 2020: GLOBOCAN estimates of incidence and mortality worldwide for 36 cancers in 185 Countries. *CA Cancer J Clin.* 2021;71(3):209-249.
doi: 10.3322/caac.21660
- Wang X, Xia C, Wang Y, *et al.* Landscape of young breast cancer under 35 years in China over the past decades: A multicentre retrospective cohort study (YBCC-Catts study). *EClinicalMedicine.* 2023;64:102243.
doi: 10.1016/j.eclinm.2023.102243
- Chinese Society of Clinical Oncology, Experts Committee on Breast Cancer, China Anti-Cancer Association, the Society of Breast Cancer, Chinese Medical Association, Chinese Society of Breast Surgery. [Expert consensus on the diagnosis and treatment of young breast cancer in China (2022 Edition)]. *Zhonghua Yi Xue Za Zhi.* 2023;103(6):387-403.
doi: 10.3760/cma.j.cn112137-20220907-01895
- Mokhtary A, Karakatsanis A, Valachis A. Mammographic density changes over time and breast cancer risk: A systematic review and meta-analysis. *Cancers (Basel).* 2021;13(19):4805.
doi: 10.3390/cancers13194805
- Hussein H, Abbas E, Keshavarzi S, *et al.* Supplemental breast cancer screening in women with dense breasts and negative mammography: A systematic review and meta-analysis. *Radiology.* 2023;306(3):e221785.
doi: 10.1148/radiol.221785
- Glechner A, Wagner G, Mitus JW, *et al.* Mammography in combination with breast ultrasonography versus mammography for breast cancer screening in women at average risk. *Cochrane Database Syst Rev.* 2023;3(3):CD009632.
doi: 10.1002/14651858.CD009632.pub3
- Gameel AM, Talaat RM, Sakr MA, Selim MA, Abo Alil DFA, Elkhoully EA. Circulating tumor DNA in Egyptian women with breast Cancer: A marker for detection of primary cases and early prediction of recurrence. *Clin Chim Acta.* 2024;562:119878.
doi: 10.1016/j.cca.2024.119878
- Li X, Dai D, Chen B, Tang H, Xie X, Wei W. Clinicopathological and prognostic significance of cancer antigen 15-3 and carcinoembryonic antigen in breast cancer: A meta-analysis including 12,993 patients. *Dis Markers.* 2018;2018:9863092.
doi: 10.1155/2018/9863092
- Osman A, Lindén M, Österlund T, *et al.* Identification of genomic binding sites and direct target genes for the transcription factor DDIT3/CHOP. *Exp Cell Res.* 2023;422(1):113418.
doi: 10.1016/j.yexcr.2022.113418
- Luo HH, Ren WY, Ye AH, *et al.* DDIT3 switches osteogenic potential of BMP9 to lipogenic by attenuating Wnt/ β -catenin signaling via up-regulating DKK1 in mesenchymal stem cells. *Aging (Albany NY).* 2024;16(18):12543-12558.
doi: 10.18632/aging.206091
- Chen P, Chen C, Hu M, *et al.* S-allyl-L-cysteine protects hepatocytes from indomethacin-induced apoptosis by attenuating endoplasmic reticulum stress. *FEBS Open Bio.* 2020;10(9):1900-1911.
doi: 10.1002/2211-5463.12945
- Berastegui N, Ainciburu M, Romero JP, *et al.* The transcription factor DDIT3 is a potential driver of dyserythropoiesis in myelodysplastic syndromes. *Nat Commun.* 2022;13(1):7619.
doi: 10.1038/s41467-022-35192-7
- Wang S, Zhang M, Liu Z, *et al.* Relationship between CHOP/GADD153 and unstable human carotid atherosclerotic plaque. *Br J Neurosurg.* 2017;31(6):648-652.

- doi: 10.1080/02688697.2017.1327016
15. Scapa JV, Cloutier JM, Raghavan SS, Peters-Schulze G, Varma S, Charville GW. DDIT3 immunohistochemistry is a useful tool for the diagnosis of myxoid liposarcoma. *Am J Surg Pathol*. 2021;45(2):230-239.
doi: 10.1097/PAS.0000000000001564
 16. Zhan W, Chen L, Liu H, *et al*. Pcsk6 deficiency promotes cardiomyocyte senescence by modulating ddit3-mediated ER stress. *Genes (Basel)*. 2022;13(4):711.
doi: 10.3390/genes13040711
 17. Tyler R, Wanigasooriya K, Taniere P, *et al*. A review of retroperitoneal liposarcoma genomics. *Cancer Treat Rev*. 2020;86:102013.
doi: 10.1016/j.ctrv.2020.102013
 18. De Vreeze RS, De Jong D, Tielen IH, *et al*. Primary retroperitoneal myxoid/round cell liposarcoma is a nonexisting disease: An immunohistochemical and molecular biological analysis. *Mod Pathol*. 2009;22(2):223-231.
doi: 10.1038/modpathol.2008.164
 19. Garcia-Ortega DY. Comprehensive treatment strategy for improving surgical resection rate of retroperitoneal sarcomas: A histology-specific approach narrative review. *Front Oncol*. 2024;14:1432900.
doi: 10.3389/fonc.2024.1432900
 20. Yu Q, Zhao J, Yang A, Li X. MLLT6/ATF2 axis restrains breast cancer progression by driving DDIT3/4 expression. *Mol Cancer Res*. 2024;22(9):796-811.
doi: 10.1158/1541-7786.MCR-23-0648
 21. Zhang L, Wang Q, Wang L, *et al*. OSskcm: An online survival analysis webserver for skin cutaneous melanoma based on 1085 transcriptomic profiles. *Cancer Cell Int*. 2020;20:176.
doi: 10.1186/s12935-020-01262-3
 22. Lee CY, Lee MG, Choi KC, Kang HM, Chang YS. Clinical significance of GADD153 expression in stage I non-small cell lung cancer. *Oncol Lett*. 2012;4(3):408-412.
doi: 10.3892/ol.2012.768
 23. Zhang X, Zhou T, Li W, Zhang T, Che N, Zu G. Clinicopathological and prognostic significance of C/EBP homologous protein (CHOP) in advanced gastric cancer. *Pathol Res Pract*. 2018;214(8):1105-1109.
doi: 10.1016/j.prp.2018.06.005
 24. Lin H, Liu S, Gao W, Liu H. DDIT3 modulates cancer stemness in gastric cancer by directly regulating CEBPβ. *J Pharm Pharmacol*. 2020;72(6):807-815.
doi: 10.1111/jphp.13243
 25. Jung KJ, Min KJ, Bae JH, Kwon TK. Carnosic acid sensitized TRAIL-mediated apoptosis through down-regulation of c-FLIP and Bcl-2 expression at the post-translational levels and CHOP-dependent up-regulation of DR5 Bim and PUMA expression in human carcinoma caki cells. *Oncotarget*. 2015;6(3):1556-1568.
doi: 10.18632/oncotarget.2727
 26. Li T, Su L, Lei Y, Liu X, Zhang Y, Liu X. DDIT3 and KAT2A proteins regulate TNFRSF10A and TNFRSF10B expression in endoplasmic reticulum stress-mediated apoptosis in human lung cancer cells. *J Biol Chem*. 2015;290(17):11108-11118.
doi: 10.1074/jbc.M115.645333
 27. Yang C, Xu X, Dong X, *et al*. DDIT3/CHOP promotes autophagy in chondrocytes via SIRT1-AKT pathway. *Biochim Biophys Acta Mol Cell Res*. 2021;1868(9):119074.
doi: 10.1016/j.bbamcr.2021.119074
 28. Mukherjee S, Bandyopadhyay SS. Phorbol-12-myristate-13-acetate (PMA) mediated transcriptional regulation of Oncostatin-M. *Cytokine*. 2016;88:209-213.
doi: 10.1016/j.cyto.2016.09.006
 29. Park JS, Lim CJ, Bang OS, Kim NS. Ethanolic extract of *Descurainia sophia* seeds sensitizes A549 human lung cancer cells to TRAIL cytotoxicity by upregulating death receptors. *BMC Complement Altern Med*. 2016;16:115.
doi: 10.1186/s12906-016-1094-0
 30. Li M, Thorne RF, Shi R, *et al*. DDIT3 directs a dual mechanism to balance glycolysis and oxidative phosphorylation during glutamine deprivation. *Adv Sci (Weinh)*. 2021;8(11):e2003732.
doi: 10.1002/advs.202003732
 31. Lopez-Bergami P, Lau E, Ronai Z. Emerging roles of ATF2 and the dynamic AP1 network in cancer. *Nat Rev Cancer*. 2010;10(1):65-76.
doi: 10.1038/nrc2681
 32. Giannoudis A, Malki MI, Rudraraju B, *et al*. Activating transcription factor-2 (ATF2) is a key determinant of resistance to endocrine treatment in an *in vitro* model of breast cancer. *Breast Cancer Res*. 2020;22(1):126.
doi: 10.1186/s13058-020-01359-7

Appendix

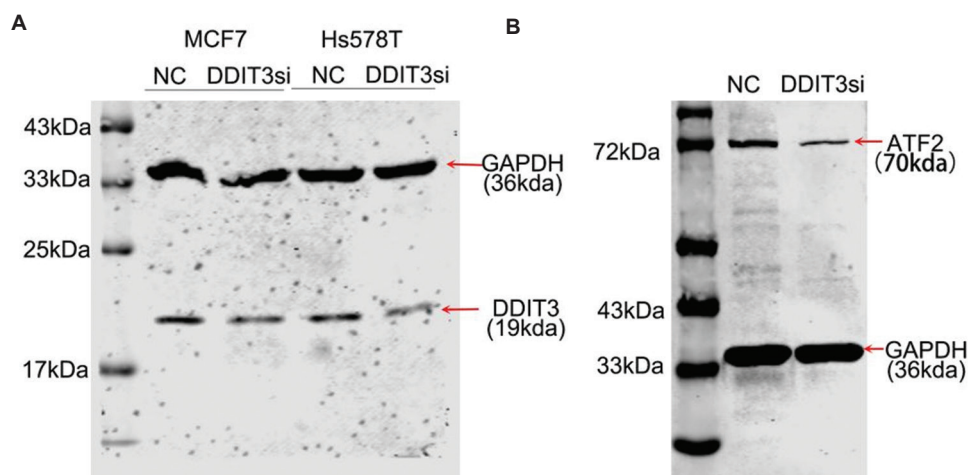


Figure A1. Original Western blot images for DNA damage-inducible transcript 3, activating transcription factor 2 (*ATF2*), and glyceraldehyde-3-phosphate dehydrogenase (*GAPDH*) corresponding to Figures 4 and 5. (A) Western blot for *DDIT3* (19 kDa) and loading control *GAPDH* (36 kDa). (B) Western blot for *ATF2* (70 kDa) and loading control *GAPDH* (36 kDa).